Low-Frequency MTF Estimation for Digital Imaging Devices Using Slanted Edge Analysis

Don Williams and Peter D. Burns
Eastman Kodak Company, Rochester, NY USA 14650-1925

ABSTRACT

Modulation transfer function (MTF) metrology and interpretation for digital image capture devices has usually concentrated on mid- to high-frequency information, relative to the half-sampling frequency. These regions typically quantify characteristics and operations such as sharpening, limiting resolution, and aliasing. However, a potential wealth of low-frequency, visually significant information is often masked in existing measurement results because of spatial data truncation. For print or document scanners, this influences measurements in the spatial frequency range of 0 to 2.0 cycles/mm, where the effects of veiling flare, micro flare, and integrating cavity effect (ICE) often manifest themselves. Using a form of edge-gradient analysis based on slanted edges, we present a method for measurement of these characteristics. By carefully adapting this well-established technique, these phenomena can be quantified. We also show how, in many cases, these effects can be treated as other spread-function or device-MTF components. The theory and field metrology of several devices using the adapted technique are also presented.

Keywords: MTF, flare, slanted edge

1. INTRODUCTION

When presented with modulation transfer function (MTF) measurements of an imaging system, one typically evaluates the magnitude and morphology of the mid- to high-spatial frequencies as indicators of imaging performance. This is where limiting resolution and sharpening effects tend to manifest themselves. Often measurements in this spatial frequency region are unremarkable, being slow to vary and bounded by unity at zero frequency. In this case, low-frequency MTF results may be seen as merely the necessary trip through the prairie before arrival at the more informative data beyond. Current MTF measurement practices, however, often mask, or are influenced by, imaging characteristics such as optical flare of various kinds, e.g., integrating cavity effect (ICE).[1]

We first address the bias introduced into current MTF measurements by optical flare, which is not usually included in such evaluations. From analysis of this error, it is possible to obtain a spatial frequency-based measure of the effective flare introduced by an image acquisition system. The key to accomplishing this is a sufficiently long data record length, which can reveal low-frequency MTF trends. Edge-gradient analysis is ideally suited to this task because of the ease with which uninterrupted data can be interpreted. Slanted-edge analysis was used here because of its insensitivity to feature alignment and its established use for digital scanning devices.

2. MEASUREMENT THEORY

The theory behind edge gradient analysis for MTF metrology is well established [2-4] and its application to digital capture devices via slanted edges is also well documented [5,6] and part of an ISO standard.[7] Edge-gradient analysis is a line spread function (LSF) transformation technique that derives the LSF, *l(x)*, through the first derivative of the edge spread function (ESF), *e(x)*:

$$l(x) = \frac{d(e(x))}{d(x)}. \tag{1}$$

The MTF is calculated by,

$$MTF(\nu) = \left| \int_{-\infty}^{+\infty} l(x) \exp(-i2\pi\nu x) dx \right|. \tag{2}$$

It should be noted that in Eqs. 1 and 2, the ESF is assumed to be the image of an ideal input-edge signal (exposure). For practical systems, if the input-edge feature used is of sufficiently high optical quality, in terms its edge modulation, the above modulus of Eq. 2 can be taken as the MTF of the system whose output provided the data. If this is not the case, the output modulation divided by the input target modulation frequency-by-frequency yields the system MTF. When no account is taken of the input-edge modulation, the measured modulus can still provide a useful measurement relative to the input-target edge and other relevant operating conditions. We will refer to the result based on a single measurement as a spatial frequency response (SFR) and one corrected for the input modulation as an MTF.

An additional assumption of Eq. 2 is that the integral of the LSF is unity, which, by Fourier transform properties results in the zero-frequency value, $MTF(0) = 1$. In practice, the resulting measured MTF is usually rescaled by a constant so that the zero-frequency condition is met. An outline of the common steps used in edge-gradient analysis is shown in Fig. 1, where the input data is taken in units of effective exposure. The currently used slanted-edge MTF method is similar to traditional edge-gradient methods, but the first step of edge-profile estimation has several component operations for finding the location and slope of the edge, etc. More details are available in Fig. 2 of Reference 6.

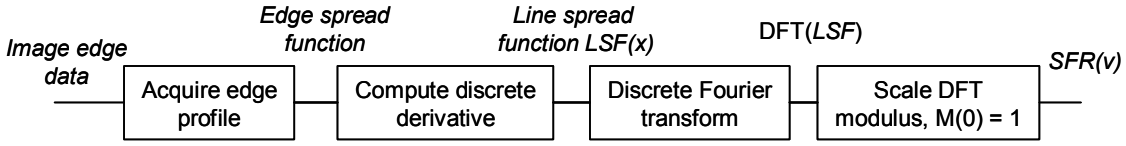

Figure 1. Steps in the edge-gradient method

The above description of MTF, or SFR, estimation makes no mention of finite image data extent, but assumes that the entire edge, and therefore line spread function, has been acquired. Because all practical measurements involve limited input data, Eq. 2 is often modified to accommodate integrating over finite limits*

$$\hat{MTF}(\nu) = \left| \int_{-a/2}^{+a/2} l(x) \exp(-i2\pi\nu x) dx \right| \tag{3}$$

where the input data is of length a. Analysis of any errors introduced by this 'data window is commonly done by defining a *rect* (rectangle) function,

$$\begin{aligned} rect(ax) &= \frac{1}{a}, \frac{-a}{2} \le x < \frac{a}{2}. \\ rect(ax) &= 0, otherwise \end{aligned} \tag{4}$$

within the integral of Eq. 3 expressed as

$$\hat{MTF}(\nu) = \left| \int_{-\infty}^{+\infty} l(x) rect(ax) \exp(-i2\pi\nu x) dx \right|. \tag{5}$$

* The continuous form of estimate is used here; however, for sampled data, corresponding discrete equations apply.

By Fourier transform properties, the multiplication of *l(x)* by the *rect* function is equivalent to a convolution of the ideal MTF and the Fourier transform of *rect*(*ax*) in the spatial frequency domain. The Fourier transform of the *rect* function is

$$\Im\big(rect(ax)\big) = \mathrm{sinc}(\nu / a) = \frac{\sin(\pi\nu / a)}{\pi\nu / a},$$

therefore,

$$\hat{MTF}(\nu) = MTF(\nu) \otimes \mathrm{sinc}(\nu/\mathrm{a}) . \tag{6}$$

$\Im(\ )$ indicates Fourier transform, and $\otimes$ convolution. Figure 2 shows several of these *sinc* spectral windows, where *n* is the number of data. This corresponds to the width of the input data area in pixels for the slanted-edge analysis of a vertical edge.

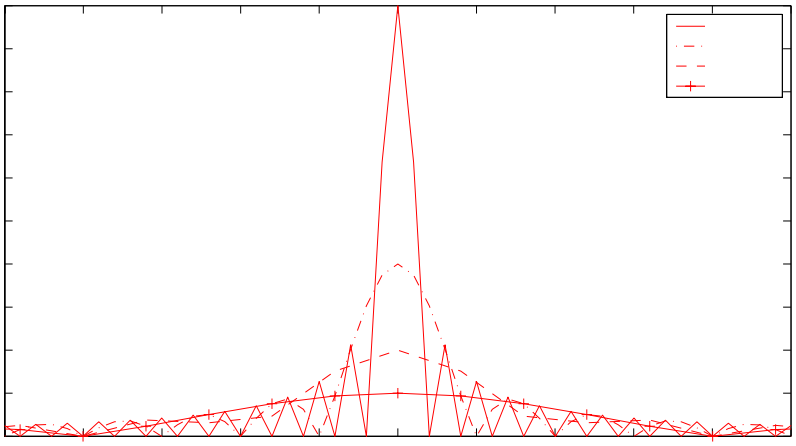

Figure 2. Spectral windows for several discrete record lengths, n, where $a = n\ dx$, and dx = sampling interval

The convolution operation of Eq. 6 gives rise to a smoothing of the measured SFR, which is commonly used in signal processing. The convolution, however, is circular, as implied by the spatial frequency axis of Fig. 2. Since measured edge SFRs are decreasing functions of spatial frequency, the finite data length can also apply a negative bias to the estimated SFR at low spatial frequencies. This is particularly true when the underlying line-spread function is wide, because of, e.g., optical flare. We illustrate this by example.

A desktop scanner was used to acquire a scan of a high quality edge target made from two butting sheets of uniform material. The image data, transformed to be proportional to paper reflectance, were used as input to the slanted-edge analysis. In this case, however, the final step was modified so that the measured SFR results were normalized to the area under the longest LSF, for n = 500. Figure 3 shows the results for several values of n. For this particular scanner, an upturn in SFR was observed near zero frequency for n = 500. As described above, however, the effective spectral window for lower values of n reduced this low-frequency component. To see the resulting effect of the data length when the standard slanted-edge analysis was applied, the scaling procedure of Fig. 1 was followed. Because the negative bias evident in Fig. 3 was most pronounced at and near zero frequency, the scaling step in the MTF measurement introduced a *positive* bias into most of the resulting SFR data. Note that the measured results show the reduced frequency sampling, and smoothing effects, expected with sampled data systems and window-induced smoothing.

The effect of reduced data windows for systems that exhibit such low-frequency characteristics is to mask such details in the resulting SFR or MTF. That the slanted-edge analysis is sensitive to this windowing, however, suggests that by varying analysis conditions, it may be possible to detect such performance characteristics, whether resulting from flare or not, while reducing the bias introduced by the final scaling step.

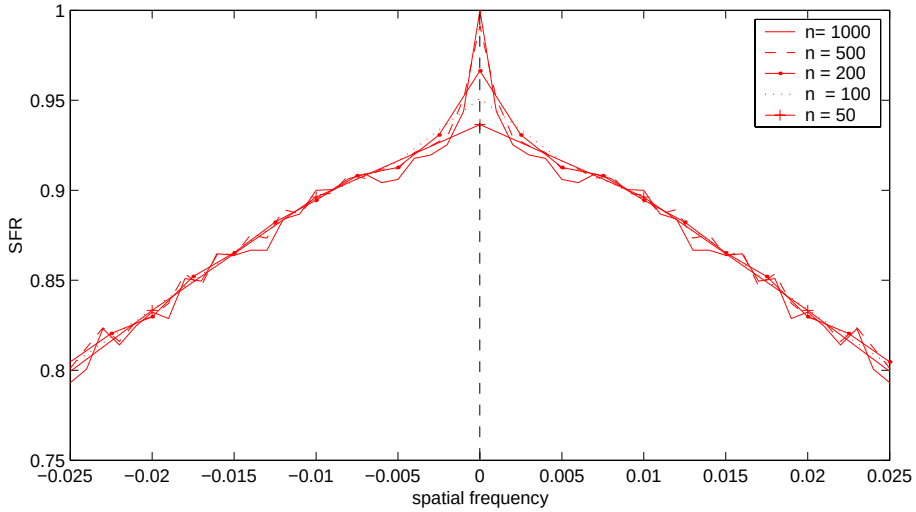

Figure 3. Measured SFR for various data lengths and scaling as per largest set. Spatial frequency is in cy/pixel

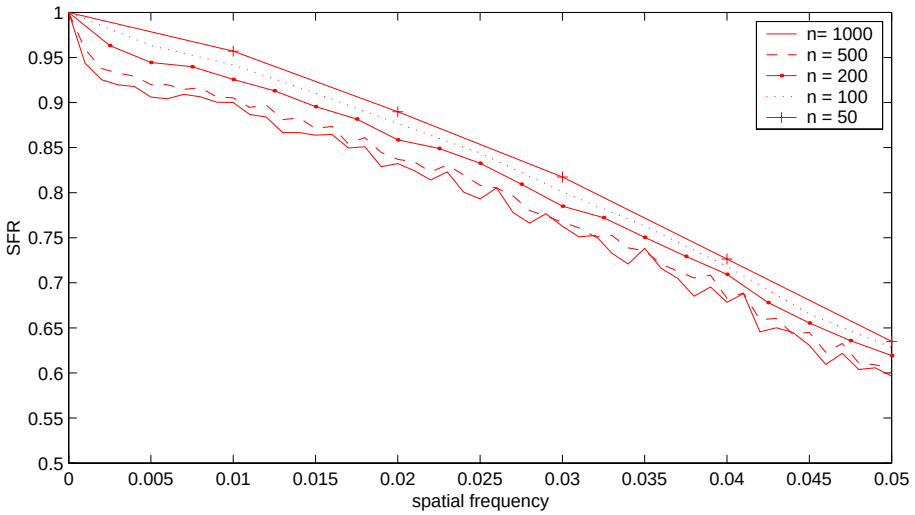

Figure 4. Result of edge data truncation of the slanted-edge SFR with normal scaling

3. EXPERIMENTAL

3.1 Introduction

Demonstrating the utility of MTF as a suitable metrology tool for estimating a single-valued flare metric is one goal of this paper. A comparison between traditional flare metrology and MTF metrology was performed to accomplish this. Two different targets were used. One, depicted in Fig. 5, is a traditional target format used to measure flare in optical imaging systems: a dark patch with a white surround (RHS) and the same density patch in a dark surround (LHS). The overall dimensions of the target were 100 mm x 150 mm. A single-valued measure of flare can be calculated by comparing the measured reflectances of the two, centered dark patches of each half of the target. The patch sizes were 6.0 mm in diameter. The measured patch reflectance in the dark surround, R_o, can be considered the zero-flare reference, while that in the light surround, R_f , is compared to it for a measure of flare. The measured reflectance difference

between these two patches divided by the target's reflectance range gives the flare value. This is given by Eq. 7. The multiple dark patches surrounding the center patch of the LHS are used to build a digital count-to-reflectance look-up table for calculating the effective measured reflectance of R_f.

$$\% \, Flare = 100 \frac{R_f - R_o}{R_o - R_{\max}} \tag{7}$$

where: R_o = Reflectance of zero-flare aim patch
R_f = Effective patch reflectance measured in light surround
R_{max} = Reflectance of light surround

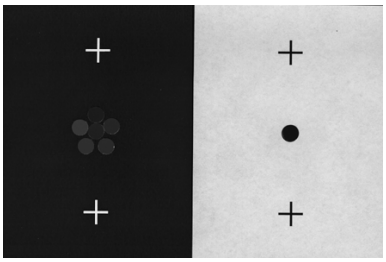

Figure 5. Traditional flare target

Figure 6. Low-contrast slanted-edge target

The second target, shown in Fig. 6, is suitable for edge-gradient analysis. It was created by mechanically butting two neutral Munsell patches. While this technique does not ensure a high bandwidth target, it minimizes low-frequency effects from optical target creation techniques – perfect for this experiment. This target measured 50 mm x 100 mm and was created in both low- and high-contrast versions. The former had optical densities of 0.26 and 0.60, and the latter 0.11 and 1.33. The intent of measuring with different contrast targets was to determine whether similar results would be observed with both, indicating that the proposed flare method is consistent with a linear-systems approach supported by the low spatial frequency measurement techniques of Section 2. Furthermore, the targets of Figs. 5 and 6 were meant to complement each other by providing a means of comparison with existing integrated techniques.

To minimize the confounding influences of radiometric nonuniformities, only flatbed reflection scanners were considered for evaluation. Their tendency to exhibit integrating cavity effect was also a factor. The scanner selection was based on perceived imaging performance prior to testing, with the goal of choosing units with a variety of low-frequency MTF performance. For simplicity, only the green image record was evaluated and acquired with 16-bit signal quantization proportional to reflectance data at 300 dpi. A Photometric Data Systems (PDS) microdensitometer was used as a benchmark scanner.

3.1 MTF results

To reduce low-frequency MTF estimation errors associated with data length truncation, unusually long regions of interest (ROI) measuring 60 mm x 10mm were chosen from the scans of the slanted-edge targets. From these ROIs, SFRs were calculated, which were consistent with the protocols defined in ISO 16067-1. For comparison, SFRs estimated from narrower but normally sized ROI widths (4mm x 10 mm) were also calculated. Example SFRs from Scanner A, illustrating the pronounced difference in low-frequency behavior under these different windowing conditions, are given in Fig. 7. Shown are the responses for both the high- and low-contrast targets. These are accompanied in the log-linear plot of Fig. 8 with their equivalent LSF. The shaded area in the center of Fig. 8 indicates the window length associated with the narrower width ROI. The entire width represents the long window length.

Note how the LSF continues to fall, almost two orders of magnitude, beyond the short window length limits. It is the long tails of the LSF that contribute to the depressed low-frequency behavior of the MTFs, which are a more accurate estimation of the true MTFs of the scanner systems.[10] We emphasize that the fall-off behavior of Fig. 8 is not an artifact of illumination or target nonuniformity. The experiment was carefully planned to eliminate these possibilities.

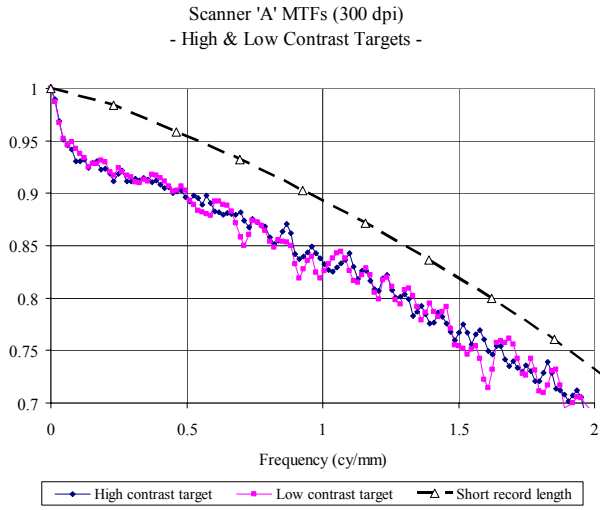

Figure 7. Scanner A MTFs

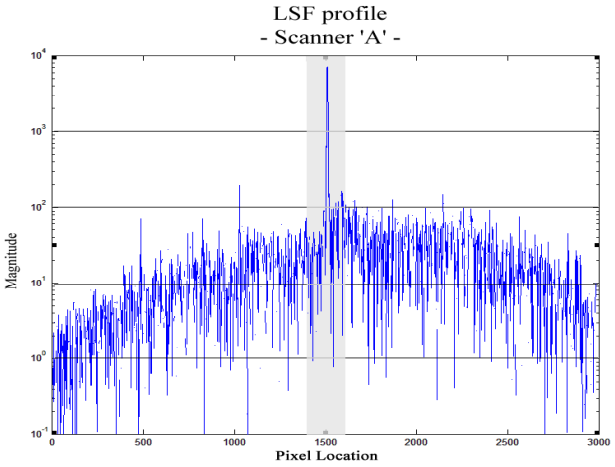

Figure 8. Scanner A, LSF profile

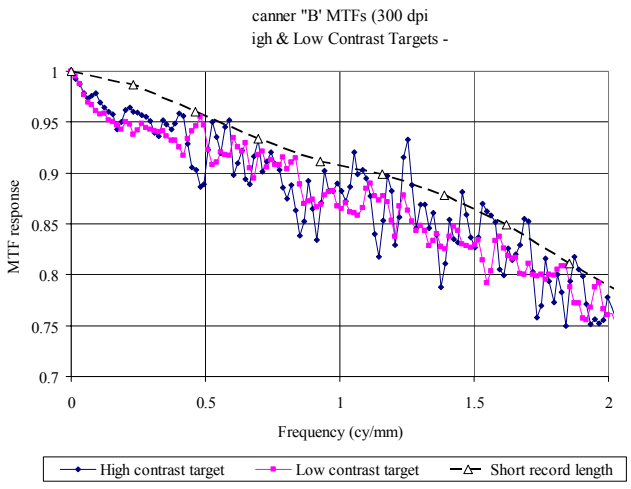

Figure 9. Scanner B MTFs

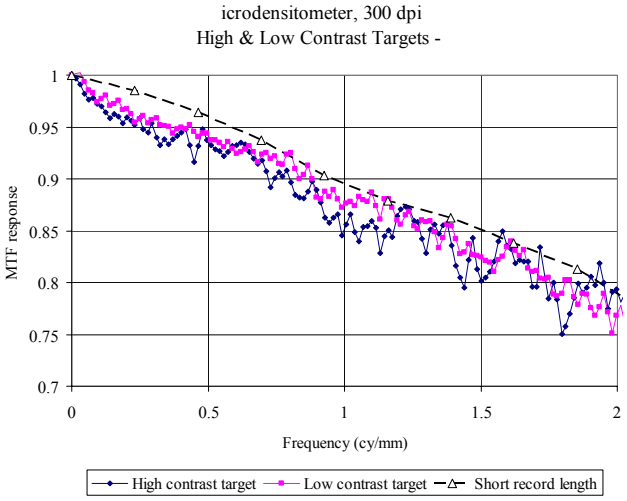

Figure 10. Microdensitometer MTFs

As Figs. 7, 9, and 10 illustrate, there is effectively no difference in the MTF estimates for data collected with the high- and low-contrast targets. This is a strong indication that the low-frequency MTF behavior is governed by linear operators and is independent of signal amplitude. The less pronounced low-frequency characteristics associated with the microdensitometer and Scanner B* are quantitative indicators of lower flare, compared with Scanner A.

3.2 Single-valued flare metrology

The benefit of frequency domain analysis in assessing imaging performance is well established. By providing a simple contextual architecture to evaluate the influence of imaging system components, including the viewer, it often enables a higher, more unified level of imaging understanding than space domain approaches. For quality control purposes, though, one often wishes to translate the multi-valued nature of MTFs into a single-valued pass/fail criterion. For instance, acutance metrics[11] successfully integrate the product of an imaging system's MTF and the visual contrast

* This sentence has been edited to correct an error in the published SPIE Proceedings version of this paper.

transfer function to arrive at a single-valued sharpness metric. Traditionally, such frequency domain techniques have not been adopted for flare measurement. Instead, space domain metrics, as described in Section 2, have been used. In this section, we attempt to exploit the MTFs of Section 4 to arrive at single-valued flare metrics suitable for quality control purposes. Two different methods were chosen to calculate such metric. A comparative approach was taken for both, consistent with the dark patch method of Section 2. Recall from Eq. 7, the difference between a zero-flare aim, R_o, and a finite flare value, R_f, was scaled by the total signal range. A similar approach was taken here and is described next.

The first method is a zero-frequency estimation approach and is proportional to the amount of energy excluded from the LSF through premature truncation. The flare magnitude, *F(0)*, is estimated by evaluating the zero-frequency component of the MTFs for both large, *N*, and small, *n*, record lengths, – both scaled with respect to the area under the LSF associated with longer window's record length (see Fig. 3). The narrow window was chosen to be 1.5% as wide as the larger one and is consistent with the window dimensions of Section 3 at 300 dpi sampling. The difference in the zero frequency component estimates for the two window sizes was used as a single-valued measure of flare and is formulated in Eq. 8.

$$F(0) = 1 - \hat{MTF}_{n/N}(0) \tag{8}$$

where: $\hat{MTF}_{n/N}(0) \equiv \hat{MTF}_n(0)$ as scaled by $\int_{-N/2}^{+N/2} l(x)dx$.

A comparison for the dark patch method of Section 2 and the above zero-frequency approach is given in Fig. 11. Data for four different scanners at both target contrast levels are shown. The correlation between the two techniques, assuming a linear model, is $R^2 = 0.83$. The consistently lower estimates for the high-contrast targets compared to the low-contrast targets were inexplicable, especially when compared to the other method described next.

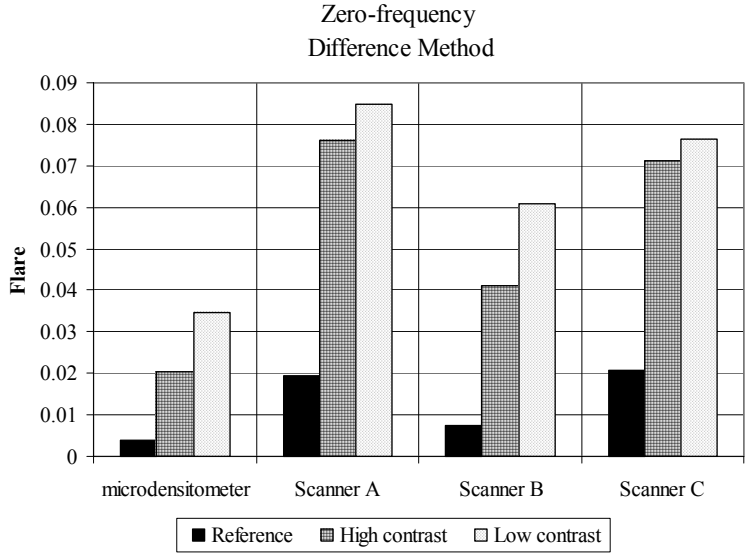

Figure 11. Single-value flare results for zero-frequency method

MTF integration, similar to acutance, formed the other investigated metric. Having at hand the MTF estimates for a wide spatial window, $\hat{MTF}_N(v)$ and a narrower one, $\hat{MTF}_n(v)$, the areas under these responses are calculated with respect to a designated frequency bandwidth, ω, and formulated as F_i according to Eq. 9. Here, $\hat{MTF}_n(v)$ is taken as describing the zero-flare condition.

$$F_i = \frac{\int_0^{\omega} M\hat{T}F_n(v)d(v) - \int_0^{\omega} M\hat{T}F_N(v)d(v)}{\int_0^{\omega} M\hat{T}F_n(v)d(v)} \tag{9}$$

The frequency bandwidth for this experiment was chosen to be 0.18 cy/mm to approximate the spatial frequency extent of the circular 6.0 mm target features of Fig. 5. The results for this method were similar to the previous one and are illustrated in Fig. 12. Slightly better correlation ($R^2 = 0.91$) between the dark patch approach and this one were noted. There was also better agreement between results for the different target contrasts with no significant difference between them.

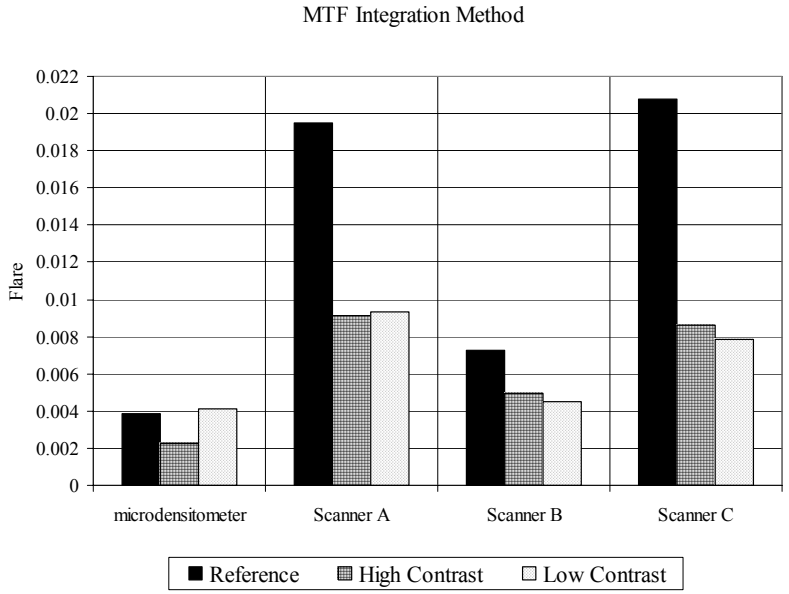

Figure 12. MTF integration results for ω = 0.18 cy/mm

It is difficult to draw strong conclusions from such limited data sets, but it is clear that significant correlations between the dark patch method and the MTF approaches shown here do exist. The range of scanner and target variables demonstrates this. Future improvements to the experimental methods would account for differences in two dimensional frequency responses and ROI sizes used in the dark patch method. The latter of these has historically contributed to flare metrology variability.

4. SUMMARY

We have shown how premature LSF truncation can dramatically affect low-frequency MTF estimates and have demonstrated this for different scanner types and signal strengths. Since long uninterrupted data lengths for the LSF are required for proper MTF estimation, edge targets were chosen as the obvious method for signal generation. They are also extremely easy and inexpensive to generate. The slanted-edge protocols of ISO 16067-1 were used for analysis for their ease of use, open availability, and general acceptance through various standards.

Because flare and ICE manifest themselves as low spatial frequency effects, it is appropriate to consider using MTF as a unified tool to quantify them as single-valued metrics. Using the appropriate MTF techniques described, two summary MTF-based flare metrics were demonstrated and compared with a traditional dark patch flare method. Good correlations between the proposed MTF-based methods and the traditional methods were noted.

REFERENCES

1. R. P. Herloski, Analytical Computation of Integrating Cavity Effect, *Proc. SPIE*, **3482**, 410-421, 1998.
2. F. Scott, R. M. Scott, and R. V. Shack, The Use of Edge Gradients in Determining Modulation-Transfer Function, *Photogr. Sc. and Eng*., **7**, 64-68, 1963.
3. R. A. Jones, An Automated Technique for Deriving MTFs from Edge Traces, *Photogr. Sc. and Eng*., **11**, 102-106, 1967.
4. C. J. Dainty and R. Shaw, Image Science, Academic, NY, 1974, pp. 244-246.
5. S. E. Reichenbach, S. K. Park, and R. Narayanswamy, Characterizing Digital Image Acquisition Devices*, Opt. Eng*., **30**, 170-177, 1991.
6. P. D. Burns, Slanted-Edge MTF for Digital Camera and Scanner Analysis, *Proc. PICS Conf*., IS&T, 135, 2000.
7. ISO/TC WG18, Photography – Electronic still picture cameras – Resolution measurements, ISO, 1998.
8. P. D. Burns and D. Williams, Refined Slanted-Edge Measurement for Practical Camera and Scanner Testing, *Proc. IS&T 2002 PICS Conference*, IS&T, 191-195, 2002.
9. K. Doi, K. Strubler, and K. Rossmann, Truncation Errors in Calculating the MTF of Radiographic Screen-film Systems from the Line Spread Function, *Phys. Med. Biol*, **17**, 241-250, 1972.
10. J. J. Jakubowski, Methodology for Quantifying Flare in a Microdensitometer, *Opt. Eng*., **19**, 122-131, 980.
11. G.C. Higgins, Image Quality Criteria, *J. App. Phot. Eng.,* **3**, 53-60, 1977.